ELSEVIER

Polymer 42 (2001) 8541–8547

polymer

www.elsevier.com/locate/polymer

Influence of UV radiation wavelength on conversion and temperature distribution profiles within dimethacrylate thick material during photopolymerization

L. Lecamp, P. Lebaudy*, B. Youssef, C. Bunel

Laboratoire de Matériaux Macromoléculaires, Institut National des Sciences Appliquées de Rouen, UMR CNRS 6522 Polymères, Biopolymères, Membranes, Place E Blondel, BP 08, 76131 Mont Saint Aignan Cédex, France

Received 7 October 2000; received in revised form 17 April 2001; accepted 15 May 2001

Abstract

UV-light initiation is now commonly used to induce polymerization of multifunctional monomers. The highly crosslinked networks obtained have a wide variety of applications. The thermal effects which take place during polymerization can be the cause of non-homogeneity and defects in the final material. These defects greatly alter the physical properties of the final products, particularly the optical ones, which causes problems in the design of thick and optically perfect materials. To better control the homogeneity of photocured materials and to determine the influence of different experimental parameters on them, conversion and temperature distribution profiles within a material during photopolymerization were simulated numerically, using the general heat equation applied to one-dimensional system. To describe the true conditions of kinetic experiments, some necessary parameters were measured, like conversion, reaction rate, spectral irradiance of the Hg vapor lamp and dimethacrylate spectral absorbance. We focused our attention more particularly on the influence of the irradiation wavelength. Indeed, the high values of the spectral absorbance coefficient cause a great decrease in light intensity in the depth of the material and lead in turn to a sharp drop in conversion. © 2001 Elsevier Science Ltd. All rights reserved.

Keywords: Photopolymerization; Conversion profile; Temperature profile

1. Introduction

Photoinitiated polymerization of multifunctional monomers provides an easy and rapid method for producing highly crosslinked polymer networks. The rapid cure and excellent physical properties of these networks have led to a growing demand and new applications for these materials [1–4]. Unfortunately, in the case of thick material production, the thermal effects taking place during polymerization can be the cause of defects in the final material [5,6]. These heterogeneities greatly alter the physical properties of the final products, and particularly the optical ones, which causes problems in the design of thick and optically perfect materials.

To ensure the effective use of these materials and to tailor them for a particular application, a good knowledge of conversion and temperature distribution profiles within the material during photoinitiated polymerization is essential. However, the measurement of these parameters during the process is impossible because no suitable technique is available to monitor their variations within a thick material. Moreover, it is well-known that polymerization continues after the end of irradiation [7–11]. This postpolymerization reaction is very fast during the first seconds after the end of UV radiation and continues at a lower speed later in time. Thus, even though it is possible to cut a thick material in thin slices after the end of UV radiation and to analyze them by FTIR spectroscopy, the obtained conversion values cannot be representative of the true ones at a time t and at a place x in the initial thick material. We can therefore conclude that no valid experimental measurements can be performed until optimum conversion is reached in all the material. Only the use of a suitable simulation may solve this problem.

In this paper, our approach includes two steps. The first one deals with the determination of some necessary parameters for numerical analysis. First of all, the conversion and reaction rate versus temperature and UV light intensity were measured by photocalorimetry for thin materials. At the same time, the influence of the radiation wavelength on kinetics was studied. Indeed, a previous study [12] has shown that the use of thin samples provides isothermal

---

* Corresponding author.
E-mail address: philippe.lebaudy@insa-rouen.fr (P. Lebaudy).

PII: S0032-3861(01)00353-6

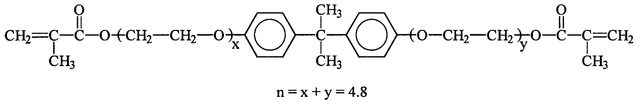

Fig. 1. Chemical formula of the dimethacrylate oligomer.

conditions, which are absolutely necessary for studying a reaction kinetic. Moreover, thin samples allow us to have a uniform illumination of the whole material and therefore to study the influence of UV light intensity on conversion carefully. Subsequently, spectral irradiance of the Hg vapor lamp and dimethacrylate spectral absorbance were performed. These measurements enable to describe the evolution of spectral radiation intensity in the sample thickness once the absorption coefficients are known.

In the second part, we describe the theoretical considerations, simplifications and assumptions which were used to carry out the simulation from the kinetic data obtained experimentally. This simulation is based on the general heat equation applied to one-dimensional system. The validity of this model to describe these photopolymerization reactions was already checked on thin materials [13]. This simulation was finally applied to the calculation of some conversion and temperature distribution profiles within a thick dimethacrylate sample to determine the influence of temperature, UV light intensity, irradiation wavelength and thickness on the structure of the final material.

2. Experimental

2.1. Materials

The chemical formula of the dimethacrylate oligomer (Akzo, $M = 575$ g mol^{-1}) used is shown in Fig. 1.

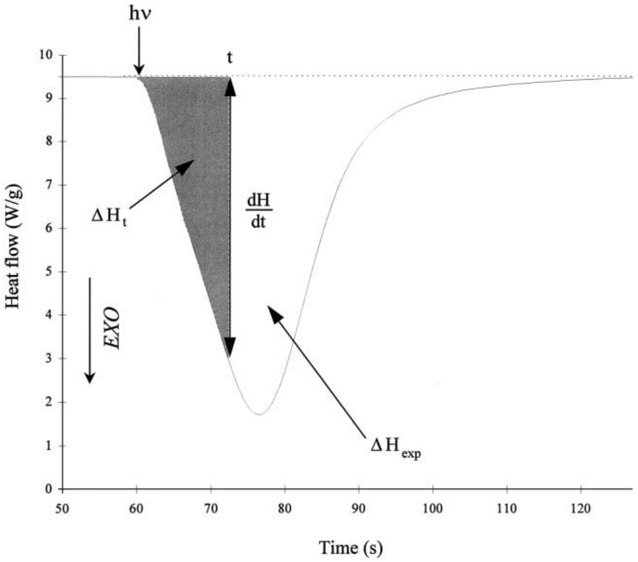

Fig. 2. Typical DSC thermogram of a photoinitiated polymerization reaction.

The photoinitiator 2,2-dimethyl-2-hydroxyacetophenone (Darocur 1173: 0.15% (w/w) i.e. 10^{-2} mol l^{-1}) was dissolved in the oligomer under stirring at room temperature for 3 h.

2.2. Photocalorimetry

About 2 mg of the mixture were placed on a polyethylene (PE) film (0.1 mm) covering the bottom of an aluminum DSC pan in order to get a maximum spreading out of the monomer as a thin and plane layer. Indeed, without PE film, a hemispherical drop is obtained and the optical disturbance can affect experimental data.

Photopolymerization kinetics were monitored by a differential scanning calorimeter (DSC 7 Perkin–Elmer) topped by an irradiation unit with two quartz windows. Heat flow versus time was recorded in an isothermal mode under nitrogen atmosphere during the photoinitiated polymerization reaction [14].

The photoinitiated polymerization has a big thermal effect, and kinetic constants are very sensitive to any increase in temperature. A previous simulation of heat transfer within a monomer film during photocrosslinking shows that our experimental conditions (thin film of 0.2 mm, $t_{1/2}$ (time to reach 50% conversion) = 15 s) are suitable to work in isothermal mode [12]. Indeed, whatever the polymerization temperature (from 30 to 90°C), the rise of temperature within the film, in the DSC oven, is always lower than 1°C.

Conversion was calculated from the overall heat at t (ΔH_t) corresponding to the dark area in Fig. 2:

$$C = \frac{\Delta H_t}{\Delta H_0^{\text{theor}}} \times 100 \tag{1}$$

where $\Delta H_0^{\text{theor}}$ is the specific enthalpy polymerization (−54.7 kJ/mol per methacrylate double bond, i.e. −190 J/g for our dimethacrylate oligomer [15]).

2.3. Optical parameters

UV-irradiation was performed with an Osram HBO 100 W mercury arc lamp (medium pressure). Its spectral irradiance (Fig. 3) was measured at a sample level by using a spectroradiometer (Intraspec II Oriel). UV light intensity can be adjusted and, for experiments under monochromatic irradiation, the selection of a spectral band was obtained with interference filters.

2.4. Physical constants

Throughout this paper, the values of material parameters such as diffusivity a, thermal conductivity λ and heat capacity C_p are assumed as constant in order to simplify numerical analysis, i.e. the expected increase in temperature and conversion evolution are supposed not to affect all these quantities. These values [5] are listed in Table 1.

The spectral absorbance of the oligomer–photoinitiator mixture (Fig. 4) was measured by using an UV–Visible

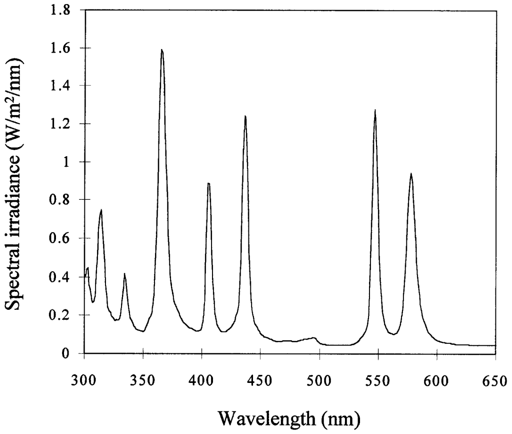

Fig. 3. Spectral irradiance of the Hg lamp.

spectrophotometer (Perkin–Elmer Lambda 16). This mixture was previously dissolved in methanol with the same concentration of monomer and photoinitiator in the solution as in the irradiated film during bulk photopolymerization.

Preliminary experiments have shown that no photopolymerization occurs at 405 nm and above. As dimethacrylate oligomer strongly absorbs below 300 nm, the photoinitiator is only efficient in the wavelength range from 300 to 380 nm (Fig. 4).

By comparison with the Hg vapor lamp spectral irradiance (Fig. 3), we notice that three main emission bands of this Hg lamp are useful. Absorption coefficient α of the mixture and molar extinction coefficient ε of the photoinitiator were determined for each main emission wavelength (Table 2).

3. Results and discussion

3.1. Kinetic results for thin materials

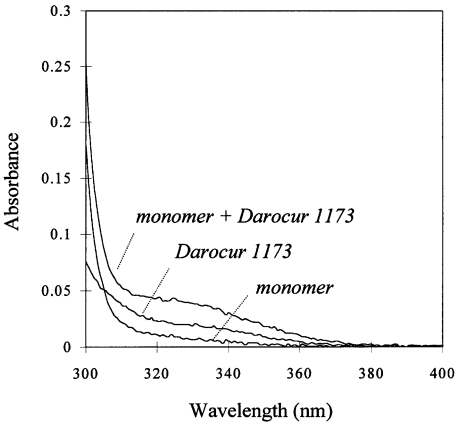

Fig. 4. Spectral absorbance of monomer, photoinitiator and the mixture.

Table 1
Physical constants of the commercial dimethacrylate

a (m^2 s^{-1})	C_p (J kg^{-1} K^{-1})	λ (W m^{-1} K^{-1})
1.616×10^{-7}	1950	0.29

Table 2
Absorption coefficient of the mixture and molar extinction coefficient of the photoinitiator

λ (nm)	313	335	365
α (m^{-1})	800	400	100
ε (l mol^{-1} m^{-1})	136	94	16

Conversion versus time was plotted (Fig. 5) at 50°C under poly and monochromatic radiation for the same intensity (2.7 mW cm^{-2}). In the case of polychromatic radiation, only the fraction of the spectral flux intensity in the range 300–380 nm is considered.

Within the limit of experimental error, the reaction kinetics are very similar for all irradiation modes. Other experiments with two other intensity values (6 and 10 mW cm^{-2}) lead to the same experimental results. This clearly shows that, whatever the radiation (mono or polychromatic), the polymerization rate and the final degree of conversion are only functions of radiation intensity and not of radiation wavelength.

In radical photopolymerization the photo-process efficiency affects the monomer conversion and the molecular weight of the polymer formed. Under condition of a steady-state in radical species the following relationship can be applied for the polymerization rate R_p:

$$R_p = \frac{k_p}{k_t^{1/2}}\sqrt{2.3\phi_i \varepsilon I_0 [A]_0}[M] \tag{2}$$

where k_p and k_t are the propagation and termination rate constants of the polymerization reaction, I_0 is the UV light intensity which is constant within a thin material, $[A]_0$ is the photoinitiator concentration, $[M]$ is the monomer

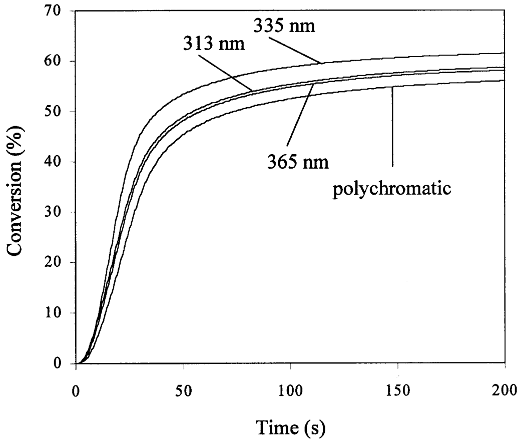

Fig. 5. Conversion versus time at 50°C for mono and polychromatic irradiation. $I_0 = 2.7$ mW cm^{-2}.

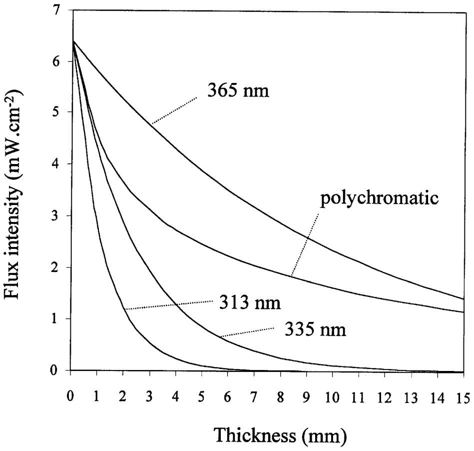

Fig. 6. Flux intensity versus thickness for mono and polychromatic irradiation. $I_0 = 6.4$ mW cm^{-2}.

concentration, ϕ_i is the initiation quantum yield and ε is the molar extinction coefficient of the photoinitiator. The factor ϕ_i takes into account the overall processes that lead to the first monomer radical RM$^{\cdot}$. It is obvious that ϕ_i will be a function of several parameters. Generally, ϕ_i is described as a product of the yields of the elementary primary processes: the quantum yield of intersystem crossing ϕ_{ST}, the yield of cleavage ϕ_α, and the yield RM$^{\cdot}$ generation $\phi_{RM^{\cdot}}$. Identical reaction rates (Fig. 5) can only be justified in Eq. (2) if the product $\phi_i\varepsilon$ is constant. As Table 2 shows, ε decreases as the irradiation wavelength increases, which means that the quantum yield ϕ_i increases with wavelength. This result, which has not been explained up to now, was already mentioned in a recent work [16], where Lovell et al. come to identical results with a different photoinitiator but with the same bandwidth.

3.2. Transposition to thick materials

In the case of thick materials, Eq. (2) is still valid for the description of reaction rates but in such cases, UV light intensity can no longer be considered as constant. For monochromatic radiation, the evolution of light intensity is described by the Beer–Lambert law, as plotted in Fig. 6 for the three main efficient wavelengths at 6.4 mW cm^{-2}.

For polychromatic radiation, the evolution of spectral radiation intensity within the material can be described by using both spectral data (Hg vapor lamp spectral irradiance and the spectral absorbance of the sample) and Beer–Lambert law.

Previous results have shown that, whatever the UV radiation wavelength, kinetic and final conversion are only functions of radiation intensity. So, it is possible to add the spectral efficiency flux within the material to obtain the total spectral flux evolution (Fig. 6). This total spectral flux was given by:

$$I(x) = \int_{\lambda_1}^{\lambda_2} I_{0\lambda}\exp^{-\alpha_\lambda x}\mathrm{d}\lambda \qquad (3)$$

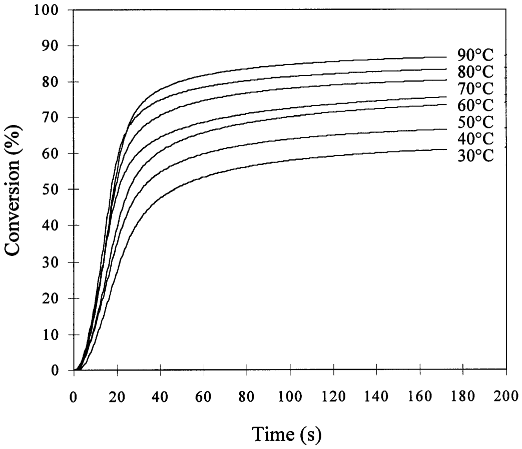

Fig. 7. Conversion versus time for temperature below 90°C under polychromatic irradiation. $I_0 = 6.4$ mW cm^{-2}.

where $I_{0\lambda}$ is the spectral flux intensity at the sample surface ($x = 0$) and α_λ is the spectral absorption coefficient of the sample ($\alpha_\lambda = \varepsilon_\lambda[A]_0$). λ_1 and λ_2 are the wavelengths delimiting the photoinitiator efficiency field.

Moreover, in the case of thick material, reaction exothermicity leads to an increase in temperature inside which modifies the reaction parameters (conversion, rate…). Therefore, we clearly see that UV light intensity and temperature variations necessarily imply a non-homogeneous material.

Only a numerical simulation can give us conversion profiles in such cases. To perform it, kinetics from different reaction temperatures and light intensities measured on thin materials are necessary.

These kinetics were measured for temperatures from 30 to 90°C and light intensity at 1.3, 3.0 and 6.4 mW cm^{-2}. Fig. 7 shows conversion versus time for a 6.4 mW cm^{-2} light intensity. The evolution of the reaction rate and ultimate conversion as a function of temperature have been discussed elsewhere [14].

3.3. Numerical simulation

3.3.1. Theoretical considerations

The numerical calculations are based on the general heat equation with two location-dependent heat sources [17]:

$$\nabla^2 T - \frac{1}{a}\frac{\partial T}{\partial t} + \frac{S(x,y,z)}{\lambda} + \frac{\Delta H_0^{\mathrm{theor}}}{aC_p}\frac{\mathrm{d}C(x,y,z)}{\mathrm{d}t} = 0 \qquad (4)$$

T is the temperature, t is the time, x,y,z is the position, $S(x,y,z)$ is the first location-dependent heat source which corresponds to the radiative flux absorption, $(\Delta H_0^{\mathrm{theor}}/aC_p)\times(\mathrm{d}C(x,y,z)/\mathrm{d}t)$ is the second location-dependent heat source induced by polymerization, where $\Delta H_0^{\mathrm{theor}}$ is the theoretical photopolymerization enthalpy, C_p is the specific heat capacity, $C(x,y,z)$ is the conversion and $\mathrm{d}C(x,y,z)/\mathrm{d}t$ is the polymerization rate.

In this form, the heat conduction equation has no obvious

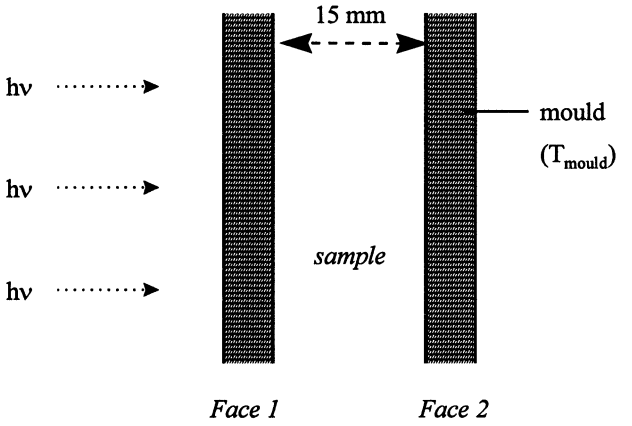

Fig. 8. Schematic shape of the experimental device.

analytical solution and the impossibility of determining accurately the boundary conditions led us to introduce some simplifications and assumptions.

3.3.2. Simplifications and assumptions

Several assumptions were made concerning the heat transfer process and reaction kinetics in a thick sheet sample:

1. Heat flow is unidirectional through the thinnest dimension of the sample (the thickness of this sheet is smaller than all other dimensions);
2. There is no flow and no molecular diffusion, so that heat is transferred only by conduction;
3. Kinetic parameters are only functions of reaction temperature and irradiation light intensity, as it was found with the photocalorimeter technique;
4. Initially, the temperature on the polymer sample faces remains the same as in the mould;
5. The slabs of the mould and sample are not in perfect contact; there is a contact thermal resistance H which is constant during the overall process ($H = 5$ W m^{-2} K^{-1}).

With these simplifications, the simulation was performed on a semi-infinite slab with 15 mm thickness between two moulds. The slab is made of an homogeneous mixture of dimethacrylate resin and photoinitiator. The UV radiation originates from a stationary light source and arrives on Face 1 (Fig. 8).

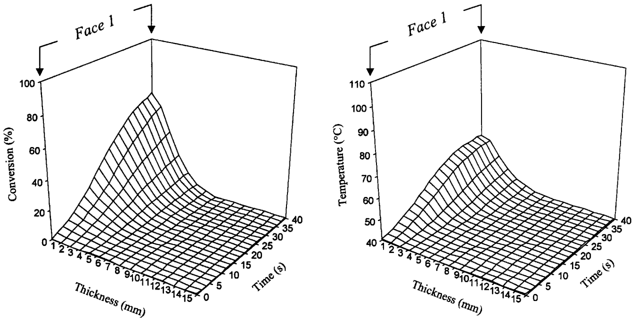

Fig. 9. Conversion and temperature distribution profiles versus time and thickness for a 313 nm wavelength.

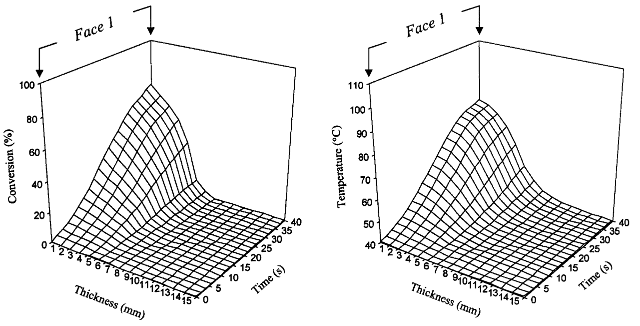

Fig. 10. Conversion and temperature distribution profiles versus time and thickness for 335 nm wavelength.

Thus, the heat conduction Eq. (5) is simplified and given by:

$$\frac{\partial^2 T}{\partial x^2} - \frac{1}{a}\frac{\partial T}{\partial t} + \frac{S(x)}{\lambda} + \frac{\Delta H_0^{\text{theor}}}{aC_{\text{p}}}\frac{\mathrm{d}C(x)}{\mathrm{d}t} = 0 \qquad (5)$$

3.3.3. Initial and boundary conditions

3.3.3.1. Initial conditions. Initially ($t = 0$), the temperature throughout the sample is assumed to have a uniform value T^0. Thus, at $t = 0$, if T_j^0 is the temperature at point j, $T_j^0 = T^0$ independently of j.

3.3.3.2. Boundary conditions. At t, the flux across the surfaces is proportional to the difference between the surface temperature T_{s}^t and the mould slabs temperature T_{mould}:

$$\frac{\partial T^t}{\partial x} = -\frac{H}{\lambda}(T_{\text{s}}^t - T_{\text{mould}}) \qquad (6)$$

where H is the contact thermal resistance.

3.3.4. Numerical analysis

Because of the internal heat generated by the reaction which is a function of time and space, Eq. (5) cannot be integrated mathematically. The problem was solved by using an explicit numerical method with finite differences [18]. In our method, we respectively replace the space-derivative $\partial^2 T/\partial x^2$ and the time-derivative $\partial T/\partial t$ in Eq. (5) by the differences $T^k_{(J+1)\ell} - 2T^k_{J\ell} + T^k_{(J-1)\ell}/\ell^2$ and $(T_\ell^{(n+1)k} - T_\ell^{nk})/k$. The physical significance of these differences corresponds to the division of the solid into slabs of thickness ℓ and the choice of an interval of time k. For convergence of the solutions and stability of the calculation, we chose the values: $\ell = 10^{-3}$ m and $k = 10^{-1}$ s for the steps in space and in time. This also allows a solution to be obtained in a reasonable number of steps.

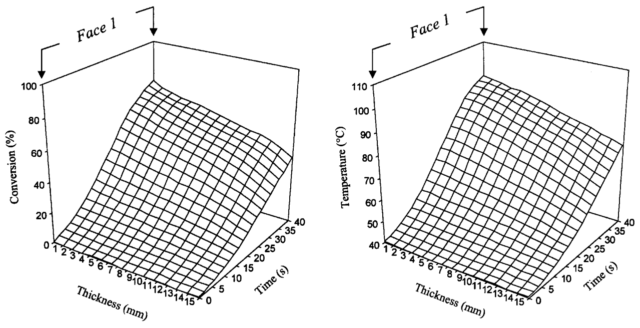

Fig. 11. Conversion and temperature distribution profiles versus time and thickness for 365 nm wavelength.

3.3.5. Calculation

The following figures present the conversion and temperature distribution profiles within a 15 mm thick dimethacrylate sample. This sample was brought to a temperature of 40°C and irradiated on Face 1 during 40 s. The only varying parameter is the radiation wavelength. UV light intensity is always 6.4 mW cm^{-2} whatever the mono or polychromatic radiation.

Figs. 9–11 show the results at 313, 335 and 365 nm, respectively. According to the evolution of spectral absorbance plotted in Fig. 6 for these three wavelengths, a notable decrease in conversion versus depth is obtained. As expected, the more homogeneous the material, the smaller the absorption coefficient is. This is very clear at 313 and 335 nm where a conversion wall is observed within the material at very small thickness.

On the other hand, by working with a polychromatic radiation (Fig. 12), the decrease in the absorption coefficient profile is much lower and therefore the conversion heterogeneity in the sample is reduced.

The temperature increase within the material results from the release of heat generated by photoinduced polymerization. Thus, because of the low thermal conductivity of the material (Table 1), the temperature distribution profile follows that of the conversion for the four irradiation modes, i.e. the more the conversion increases, the more the temperature rises and conversely. The conversion profiles obtained after 40 s of irradiation are plotted in Fig. 13. For the same incident radiation intensity (6.4 mW cm^{-2}), we notice that conversion on the material surface varies between 62 and 73%. This conversion variation can only be explained by a different evolution of surface temperature, as shown in Fig. 14.

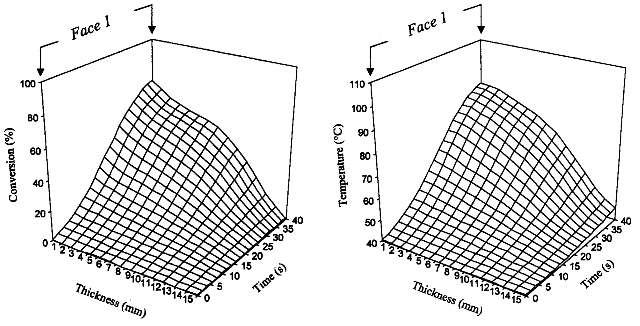

Fig. 12. Conversion and temperature distribution profiles versus time and thickness for polychromatic irradiation.

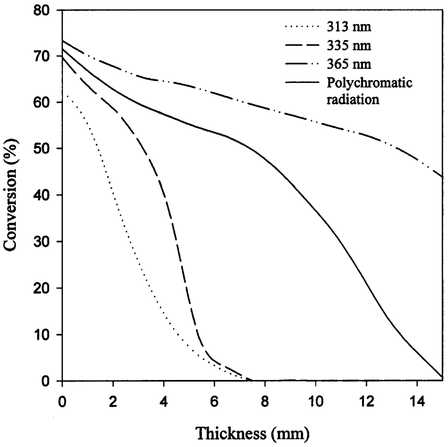

Fig. 13. Conversion profile versus thickness after 40 s of mono or polychromatic irradiation.

4. Conclusion

By means of numerical simulation and thanks to photopolymerization kinetics results obtained on thin dimethacrylate samples, the calculation of temperature and conversion profiles developed through thick dimethacrylate material was carried out for different times and irradiation modes. The influence of irradiation wavelength was more particularly investigated. We have shown therefore that, in the case of thin samples, the polymerization rate does not depend on the irradiation

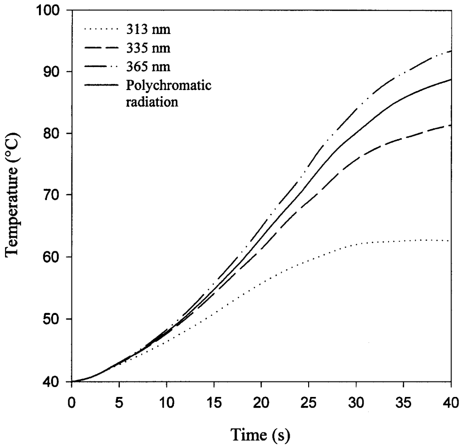

Fig. 14. Temperature evolution versus time on Face 1 for mono or polychromatic irradiation.

wavelength. However for thick materials, the increase in absorption coefficient values induces a significant decrease of the absorbed light intensity in the depth of the material and leads to a great conversion decrease. The thermal effects of fast photoinitiated polymerization also generate a significant temperature increase. For thick samples, low dimethacrylate thermal conductivity induces a low dissipation of the polymerization heat generated and, as a result, the simulated temperature distribution profile is similar to the conversion one, i.e. the greater the conversion, the higher the temperature.

This study allows us to draw conclusions about the best experimental conditions to produce thick and optically perfect materials. Thus, in our study, monochromatic radiation at 365 nm leads to the most homogeneous material. Unfortunately, monochromatic irradiation cannot be applied to an industrial process since it causes losses in both yield and efficiency. The alternative solution in order to improve material homogeneity would be to optimize $\phi_i\varepsilon$ by choosing a photoinitiator with low ε values, and to use a lamp which develops a high intensity in the photoinitiator spectral efficiency field.

References

[1] Finter J, Frischinger I, Haug T, Marton R. Rad Tech Europe Conference Proc Lyon (France) 1997;489.
[2] Anseth KS, Newman SN, Bowman CN. Adv Polym Sci 1995;122:177.
[3] Abadie MJM, Parfait A, Rouby M. Eur Polym J 1994;30:399.
[4] Cook WD. J Macromol Sci Chem 1982;17:99.
[5] Lecamp L, Lebaudy P, Youssef B, Bunel C. Macromol Symp 1999;148:77.
[6] Decker C, Elzaouk B, Decker DJMS. Pure Appl Chem 1996;A33:173.
[7] Zhu S, Tian Y, Hamielec AE, Eaton DR. Polymer 1990;31:154.
[8] Marino T, Long OL, Neckers DC. Ind Eng Chem Res 1995;34:4549.
[9] Kloosterboer JG, Lijten GFCM. Polymer 1987;28:1149.
[10] Decker C, Moussa K. Eur Polym J 1990;26:393.
[11] Lecamp L, Youssef B, Bunel C, Lebaudy P. Polymer 1999;40:6313.
[12] Lecamp L, Lebaudy P, Youssef B, Bunel C. J Therm Anal 1998;51:889.
[13] Kerbourch' P, Lebaudy P, Lecamp L, Youssef B, Bunel C. 31èmes J Calorim Anal Therm Proc Rouen (France) 2000;29.
[14] Lecamp L, Youssef B, Bunel C, Lebaudy P. Polymer 1997;38:6089.
[15] Anseth KS, Wang CN, Bowman CN. Polymer 1997;35:3243.
[16] Lovell LG, Elliot BJ, Brown JR, Bowman CN. Polymer 2001;42:421.
[17] Carslaw HS, Jaeger JC. Conduction of heat in solids. Oxford: Oxford Science Publications, 1959.
[18] De Vriendt AB. In: Morin G, editor. Transmission de la chaleur, vol. 1, Tome 2. 1987.